Title
Altered endochondral bone development in matrix metalloproteinase 13-deficient mice

Journal
Development, 131(23)

ISSN
0950-1991

Authors
Stickens, Dominique
Behonick, Danielle J
Ortega, Nathalie
et al.

Publication Date
2004-12-01

Peer reviewed

Altered endochondral bone development in matrix metalloproteinase 13-deficient mice

Dominique Stickens[1,*], Danielle J. Behonick[1], Nathalie Ortega[1], Babette Heyer[1], Bettina Hartenstein[2], Ying Yu[1], Amanda J. Fosang[3], Marina Schorpp-Kistner[2], Peter Angel[2] and Zena Werb[1,*]

[1]Department of Anatomy and Biomedical Sciences Graduate Program, University of California, San Francisco, CA 94143-0452, USA
[2]Deutsches Krebsforschungszentrum Heidelberg (DKFZ), Division of Signal Transduction and Growth Control (A100), Im Neuenheimer Feld 280, D-69120 Heidelberg, Germany
[3]University of Melbourne, Department of Paediatrics, Royal Children's Hospital, Parkville, Victoria, Australia
*Authors for correspondence (e-mail: domi@itsa.ucsf.edu; zena@itsa.ucsf.edu)

Accepted 25 September 2004

Development 131, 5883-5895
Published by The Company of Biologists 2004
doi:10.1242/dev.01461

Summary

The assembly and degradation of extracellular matrix (ECM) molecules are crucial processes during bone development. In this study, we show that ECM remodeling is a critical rate-limiting step in endochondral bone formation. Matrix metalloproteinase (MMP) 13 (collagenase 3) is poised to play a crucial role in bone formation and remodeling because of its expression both in terminal hypertrophic chondrocytes in the growth plate and in osteoblasts. Moreover, a mutation in the human *MMP13* gene causes the Missouri variant of spondyloepimetaphyseal dysplasia. Inactivation of *Mmp13* in mice through homologous recombination led to abnormal skeletal growth plate development. Chondrocytes differentiated normally but their exit from the growth plate was delayed. The severity of the *Mmp13*-null growth plate phenotype increased until about 5 weeks and completely resolved by 12 weeks of age. *Mmp13*-null mice had increased trabecular bone, which persisted for months. Conditional inactivation of *Mmp13* in chondrocytes and osteoblasts showed that increases in trabecular bone occur independently of the improper cartilage ECM degradation caused by *Mmp13* deficiency in late hypertrophic chondrocytes. Our studies identified the two major components of the cartilage ECM, collagen type II and aggrecan, as in vivo substrates for MMP13. We found that degradation of cartilage collagen and aggrecan is a coordinated process in which MMP13 works synergistically with MMP9. Mice lacking both MMP13 and MMP9 had severely impaired endochondral bone, characterized by diminished ECM remodeling, prolonged chondrocyte survival, delayed vascular recruitment and defective trabecular bone formation (resulting in drastically shortened bones). These data support the hypothesis that proper ECM remodeling is the dominant rate-limiting process for programmed cell death, angiogenesis and osteoblast recruitment during normal skeletal morphogenesis.

Key words: Collagenase, MMP, Homologous recombination, Knockout, Hypertrophic cartilage, Chondrocyte, Trabecular bone, Collagen, Aggrecan, Mouse

Introduction

Skeletal development occurs by two distinct mechanisms: intramembranous and endochondral ossification. Intramembranous ossification results from direct differentiation of mesenchymal precursors into osteoblasts, and is restricted to the clavicle and the bones of the skull. The axial and appendicular skeletons are formed by endochondral ossification, a process that is initiated during embryogenesis when mesenchymal cells condense and differentiate into chondrocytes. Chondrocytes located in the center of the cartilaginous template proliferate and go through several stages of differentiation and maturation. Each step of this process is accompanied by changes in structure and composition of ECM molecules produced by and surrounding the chondrocytes. Cellular hypertrophy marks the final step in chondrocyte differentiation, in which the cartilage ECM becomes calcified and partially degraded. Ossification begins when hypertrophic chondrocytes undergo programmed cell death and the calcified cartilage is invaded by blood vessels, osteoblasts (bone-depositing cells), osteoclasts (bone-resorbing cells) and mesenchymal precursors. The residual calcified cartilage matrix is then used as a scaffold for the deposition of mineralized bone by osteoblasts, resulting in the production of new trabecular bone. This process gradually proceeds outwards and establishes the two growth plates that separate the distal cartilaginous epiphyses from the medial bony diaphysis (for a review, see Karsenty and Wagner, 2002). Endochondral ossification is therefore unique in that it involves the remodeling and replacement of a template tissue (cartilage) with a distinct permanent tissue (bone). This process requires chondrocyte differentiation and apoptosis and remodeling of the cartilage matrix, followed by vascular invasion and formation of trabecular bone. Although these individual steps of endochondral ossification are well characterized, it remains

unclear how these are coordinated and which step is rate limiting.

Recent studies have shown that chondrocyte apoptosis per se does not lead to endochondral ossification (Colnot et al., 2001). Angiogenesis has been implicated as a crucial step (Maes et al., 2002; Vu et al., 1998; Zelzer et al., 2004); however, the accumulation of hypertrophic chondrocytes and their associated matrix in models where angiogenic stimuli have been ablated indicate that ECM degradation also fails to occur (Gerber et al., 1999). These observations lead to the hypothesis that degradation and remodeling of the cartilage matrix is essential for vascular invasion.

Remodeling of ECM components requires proteolytic breakdown, a process in which a variety of proteases have been implicated. Of particular interest are the members of the matrix metalloproteinase (MMP) family, owing to their ability to cleave aggrecan and collagens, the two most abundant ECM components of skeletal tissue. Collagen type II (Col2) is the primary fibrillar ECM component secreted by resting and proliferating chondrocytes in the growth plate, while collagen type I (Col1) is the primary ECM component secreted by osteoblasts in the trabecular bone. Col2 is crucial in establishing correct temporal and spatial organizational relationships with other matrix components such as the proteoglycans. Aggrecan is the major proteoglycan of the developing growth plate (Doege, 1999). Degradation of proteoglycans and Col2 occurs in the very last stages of chondrocyte differentiation, just prior to vascular invasion (Lee et al., 1999).

Several MMPs are collagenolytic, cleaving fibrillar collagens between amino acids 775 and 776 within their triple helical regions (Fields et al., 1987; Wu et al., 1990). The resulting 1/4 and 3/4 length cleavage fragments then denature and are degraded further by gelatinases, including MMP9 and MMP2 (Werb, 1982). Collagenolytic MMPs expressed during endochondral ossification include MMP13, MMP8 (collagenase 2) and MMP14 (MT1-MMP). A number of MMPs are able to cleave aggrecan, resulting in the exposure of cryptic epitopes within the protein. Other proteinases, including ADAMTS1, ADAMTS4 and ADAMTS5 (Abbaszade et al., 1999; Kuno et al., 2000; Tortorella et al., 1999), also cleave aggrecan, albeit at different sites than those recognized by MMPs.

Studies with transgenic mice lacking collagenolytic MMP14 (Holmbeck et al., 1999) or equipped with collagenase-resistant Col1 (Liu et al., 1995; Zhao et al., 1999) suggest that collagen cleavage and remodeling regulates bone homeostasis. However, the roles of chondrocytes and osteoblasts versus other cells in ECM remodeling have not been elucidated. Of the collagenolytic MMPs present in skeletal tissue, MMP13 is of particular interest because a mutation in human *MMP13* causes the Missouri variant of spondyloepimetaphyseal dysplasia (SEMD), a syndrome with abnormalities in development and growth of endochondral skeletal elements (Kennedy et al., 2003). MMP13 is expressed by both terminal hypertrophic chondrocytes and osteoblasts, and its substrates include both Col1 and Col2. Furthermore, MMP13 can synergize with MMP9 in degradation of collagen (Engsig et al., 2000). In this study, we generated mice deficient for MMP13 by homologous recombination in all tissues, as well as mice lacking MMP13 in a tissue-specific manner. We also generated mice deficient for both MMP13 and MMP9. Thus, we have been able to define the specific contributions of MMP13 alone and in combination with MMP9 to the rate-limiting processes during endochondral ossification.

Materials and methods

Mice and constructs

For the construction of the floxed *Mmp13* targeting vector, a genomic *Pst*I/*Sau*3A-fragment spanning a total of 7.2 kb of *Mmp13* sequences including the first six exons was used (Schorpp et al., 1995). The construct contained a *lox*P site within a *Dra*III restriction site located in intron 2 of the *Mmp13* gene. Additionally, the neomycin resistance minigene, flanked by two *lox*P sites, was introduced into an *Eco47RIII* restriction site within intron 5. The resulting targeting vector construct was linearized by cutting at the *Aat*II restriction site located within the vector backbone 3′ of the sequence homologous to *Mmp13*. Linearized DNA (25 μg) was electroporated into D3 embryonic stem cells. Homologous recombination events were identified by Southern analysis using different external probes. Eight correctly targeted ES cells were isolated and two independent clones (#42 and #44) were injected into C57/Bl6 blastocysts to generate chimeric mice. After the initial characterization mice generated from clone 42 were used for all subsequent studies.

To generate $Mmp13^{-/-}$ mice, floxed MMP13 mice were crossed to β-actin Cre mice, ensuring ubiquitous disruption of the *Mmp13* gene. The recombination of the floxed *Mmp13* alleles was analyzed by Southern blotting and northern blotting. *Col2-Cre* and *Col1-Cre* transgenic mice where the Cre recombinase is expressed under the rat Col2α1 or the *Col1α1* promoter, respectively, were generated as described elsewhere (Dacquin et al., 2002; Schipani et al., 2001).

All mice were housed in a specific pathogen free (SPF) environment and under light, temperature- and humidity-controlled conditions. Food and water were available ad libitum. The procedures for performing animal experiments were approved by the Institutional Animal Care and Use Committee, University of California, San Francisco.

Calvarial culture

Frontal and parietal calvariae from newborn to 5-day-old mice were cultured and the conditioned media collected and assayed for the presence of MMP13 as previously described (Peeters-Joris et al., 1998).

Staining of whole skeletons

Whole skeletal preparations of 2-week-old mice were prepared and stained with Alizarin Red and Alcian Blue as previously described (McLeod, 1980).

BrdU labeling/histology

A 10 mg/ml stock of bromodeoxyuridine (BrdU; Sigma, St Louis, MO) was injected intraperitoneally into 1-week-old mice at a dose of 100 μg BrdU per gram of mouse. Mice were sacrificed 1 hour after injection and bones were harvested. BrdU staining was carried out on paraffin sections using a kit according to manufacturer's directions (Zymed, South San Francisco, CA).

In situ hybridization

Paraffin sections were placed on acid-etched, TESPA-treated slides and prepared for in situ hybridization as described (Albrecht et al., 1997). Plasmids were linearized with the appropriate restriction enzymes to transcribe either sense or antisense ^{35}S-labeled riboprobes [*colIIA*1, and *colXA1* probes are described elsewhere (Albrecht et al., 1997); *Mmp2, Mmp13, Mmp14, VEGF* probes are described elsewhere (Colnot and Helms, 2001); *Mmp8* is described elsewhere (Sasano et al., 2002)]. Slides were washed at a final stringency of 65°C

in 23×SSC, dipped in emulsion, and exposed for 1-2 weeks. Slides were counterstained with Hoechst 33342.

Histological analyses and immunohistochemistry

Tissues were fixed in 4% paraformaldehyde in phosphate-buffered saline, decalcified in EDTA, paraffin embedded, sectioned at 5 μm and stained with von Kossa's stain, Safranin O/Fast Green or Picrosirius Red. Briefly, for Safranin O/Fast Green staining, deparaffinized and rehydrated sections were stained in Weigert's Iron Hematoxylin (Sigma, St Louis, MO), 0.02% aqueous Fast Green (Sigma) followed by a rinse in 1% acetic acid and 0.1% aqueous Safranin-O (Sigma). For Picrosirius Red staining, deparaffinized and rehydrated sections were stained in a 0.1% solution of Direct Red 80 (Aldrich, Milwaukee, WI) in saturated picric acid (Sigma) followed by washes in 0.5% acetic acid. Additional 5 μm paraffin sections were reacted for TRAP activity using a leukocyte acid phosphatase kit and counterstained with Methyl Green (Sigma).

For immunohistochemistry, tissues were fixed, embedded and sectioned as described above. For PECAM immunostaining, rat anti-mouse PECAM monoclonal antibody (Pharmingen, San Diego, CA) was used at a dilution of 1:50. For cleaved aggrecan immunostaining, deparaffinized, rehydrated sections were deglycosylated in chondroitinase ABC (Seikagaku Corporation, Tokyo, Japan) and rabbit anti-DIPEN polyclonal antibody (Singer et al., 1995) was used at a concentration of 0.6 μg/ml. For cleaved collagen staining, rabbit anti-Col 3/4 polyclonal antibody (Hdm Diagnostics and Imaging, Toronto, Canada) was used at a dilution of 1:800.

Micro-CT

Tibiae were dissected from 1-year-old mice and analyzed using a micro-CT system (μCT40, Scanco Medical, Bassersdorf, Switzerland). The trabeculae of tibiae bone were scanned using a Cone-Beam type scan into 240 slices with a voxel of 7×7×7 μm. Three-dimensional trabecular structural parameters were measured directly, as previously described (Jiang et al., 2003).

Results

Mice lacking MMP13 are viable

To study the role of MMP13 in development, we inactivated *Mmp13* using Cre/Lox recombination (Sauer, 1998). We first generated mice with a floxed *Mmp13* locus by incorporating loxP sites into the intronic regions flanking exons 3, 4 and 5, which encode the active site of the enzyme (Fig. 1A). To delete the floxed exons, mice homozygous for the floxed *Mmp13* allele *(*MMP13fl/fl) were crossed with mice carrying the *Cre* recombinase driven by the β-actin promoter. Intercrossing of mice heterozygous for both the floxed *Mmp13* allele and *β-actin-Cre* gave rise to homozygous *Mmp13* null (*Mmp13*$^{-/-}$) offspring with expected Mendelian distribution. Southern blot analyses confirmed that Cre-mediated deletion of the floxed exons was complete (Fig. 1B). Whereas pro-MMP13 (~57 kDa) was detected in the conditioned media from calvariae from wild-type and heterozygous mice, no MMP13 protein was detected in the conditioned media from calvariae cultured from *Mmp13*$^{-/-}$ mice (Fig. 1C), confirming that we had successfully generated MMP13-deficient mice.

Mmp13$^{-/-}$ mice showed no gross phenotypic abnormalities, were fertile and had a normal lifespan. Backcrossing of these mice onto a pure FVB/N background caused no overt difference in phenotype.

To assess which cells of the skeletal elements express *Mmp13*, in situ hybridization was performed on bones at various stages of the endochondral ossification process. At early stages (15 days post coitus, dpc), *Mmp13* was expressed in hypertrophic chondrocytes and newly recruited bone cells in the primary ossification center (Fig. 1D). Following the establishment of the growth plates, expression of *Mmp13* became restricted to only the very last rows of hypertrophic chondrocytes and the osteoblasts of the trabecular bone (Fig. 1E).

MMP13 deficiency causes altered growth plate architecture and increased trabecular bone during endochondral ossification

Staining of skeletons from *Mmp13*$^{-/-}$ animals with Alizarin Red and Alcian Blue showed that all elements appeared normal and were equivalent in length compared with wild-type littermates (Fig. 2A). For microscopic analyses, we focused on the tibiae and metatarsals, which differ with respect to the kinetics of growth plate closure. In contrast to metatarsals, which close their growth plates at about 4 weeks of age, a small part of residual growth plate cartilage remains in fully developed tibiae, separating the epiphysis from the diaphysis. At 15 dpc, metatarsals and tibiae show the first signs of the formation of a primary ossification center (Fig. 1D). At this stage, *Mmp13* mRNA is highly expressed in the late hypertrophic chondrocytes, where it colocalizes with collagen type X (Wu et al., 2001). *Mmp13* is also expressed in the newly recruited osteoblasts that migrate along the residual mineralized cartilage matrix (Gack et al., 1995; Johansson et al., 1997). Long bones of 15 dpc *Mmp13*$^{-/-}$ mice showed no obvious differences when compared with those from wild-type littermates (Fig. 2B,C). Thus, it did not appear that the initial stages of endochondral ossification were affected in the absence of MMP13.

At 17 dpc, the first visible and consistently observed differences between wild-type and *Mmp13*$^{-/-}$ skeletal elements became apparent in the tibiae. Although initial vascular invasion and establishment of the primary ossification center was normal (Fig. 2B,C), the growth plates in *Mmp13*$^{-/-}$ mice had a lengthened hypertrophic chondrocyte zone (data not shown). An expanded hypertrophic zone also became apparent in the metatarsals, but not before animals had reached 1 week of age (Fig. 2D,E). We found the severity of this phenotype to be highly bone specific, with a more marked expansion of the hypertrophic zone in the metatarsals than in the tibiae (compare Fig. 2F with 2G). The severity of the *Mmp13*$^{-/-}$ growth plate phenotype increased until about 5 weeks of age. After 5 weeks, the growth rate slowed down and, concomitantly, the hypertrophic chondrocyte population gradually returned to its normal size. By 12 weeks of age the growth plate phenotype was ameliorated (Fig. 2H,I). Interestingly, the staining of the cartilage by Safranin O reproducibly remained more intense in the mutant growth plates (Fig. 2I), suggesting that MMP13 contributes to proteoglycan turnover.

A second notable phenotype in the long bones of *Mmp13*$^{-/-}$ mice was an increase in trabecular bone. Although tibiae from 1-week-old *Mmp13*$^{-/-}$ mice showed no apparent change in trabecular bone compared with wild type, the shape of the bone spicules was irregular (Fig. 3A,B). At 3 weeks, tibiae from *Mmp13*$^{-/-}$ mice had a visible increase in trabecular bone (Fig. 3C,D). A similar increase was also visible in the metatarsals after 1 week of age (data not shown). The severity of the trabecular bone phenotype progressed with age. In

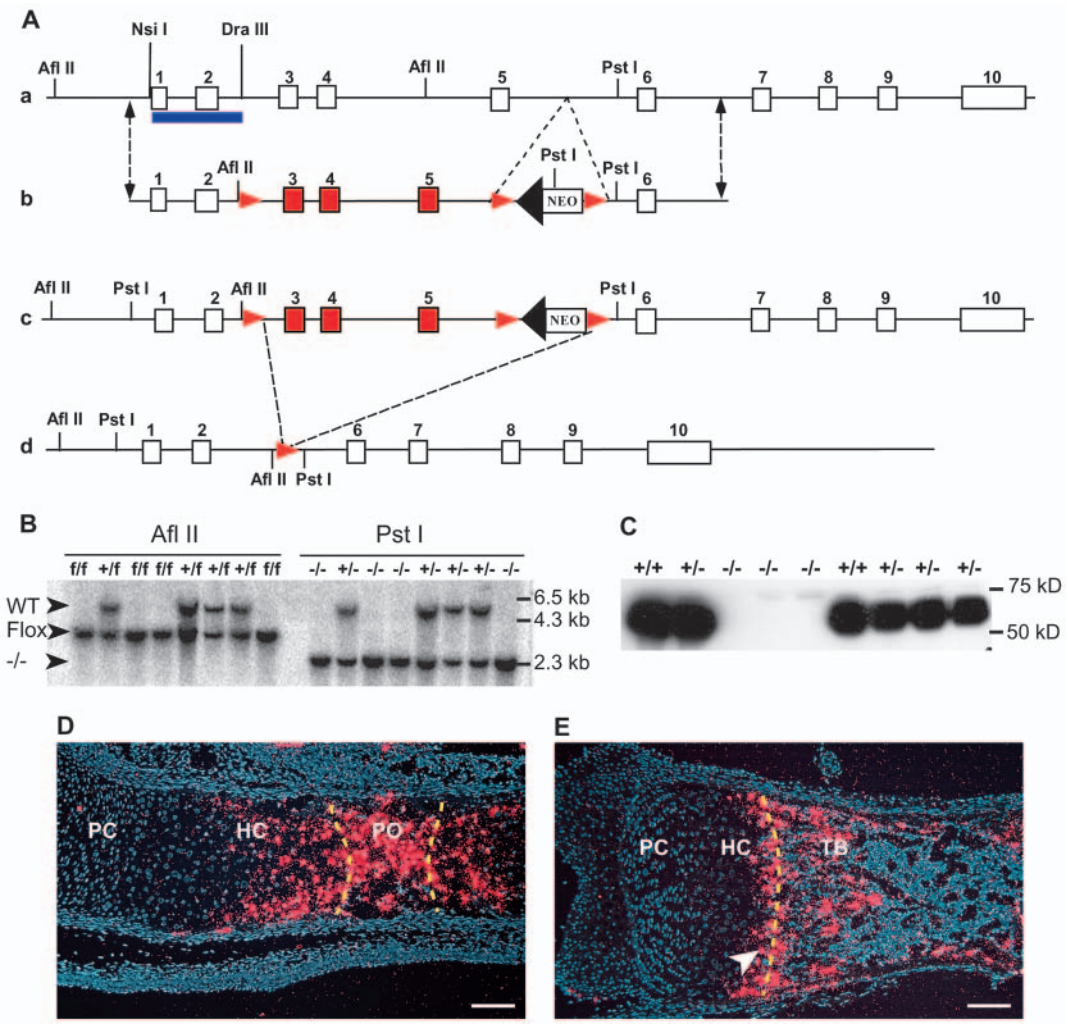

Fig. 1. Targeting of *Mmp13*. (A) Strategy for targeting of *Mmp13*. The structure of the endogenous mouse locus (a), the transgene targeting cassette (b), the targeted floxed allele resulting from homologous recombination (c) and the null allele resulting from Cre-mediated recombination (d) are depicted. Exons are depicted as open boxes; the floxed exons corresponding to the catalytic domain are shown in red. Red arrowheads indicate loxP insertion sites. Blue bar indicates probe used for Southern hybridization. (B) Southern blot analyses. Identification of MMP13fl/fl and *Mmp13*$^{-/-}$ mice by digest of genomic DNA with *Afl*II and *Pst*I, respectively. Fragments were separated according to size and hybridized to the probe indicated in A. (C) Detection of secreted pro-MMP13 in conditioned medium from mouse calvarial cultures. Conditioned medium was collected, concentrated and proteins were size fractionated. Western blot using goat polyclonal anti-pro-MMP13 shows that pro-MMP13 (57 kDa) can be detected in culture media from calvaria from wild-type (+/+) and heterozygous (+/–) animals, but not from *Mmp13*$^{-/-}$ (–/–) animals. (D) Detection of *Mmp13* expression by in situ hybridization on tibia from 15 dpc wild-type mouse. *Mmp13* signal is indicated in red. Primary front of ossification is indicated by broken yellow line. Hoechst counterstain is blue. *Mmp13* expression is observed in the hypertrophic chondrocyte population (HC) and the primary ossification center (PO), but not in the proliferating chondrocyte (PC) population. (E) Detection of *Mmp13* expression by in situ hybridization on the phalange from 1-week-old wild-type mouse. In contrast to expression pattern observed in D, *Mmp13* expression is restricted to the most terminal row of hypertrophic chondrocytes (arrowhead). TB, trabecular bone. Scale bars: 100 μm.

contrast to the expansion of the hypertrophic cartilage, however, the increase in trabecular bone persisted for months in tibiae as well as femurs (Fig. 3E-H). To confirm these histological observations, we performed micro-computed tomography (micro-CT) on tibiae from wild-type and *Mmp13*$^{-/-}$ mice. We found a dramatic and significant increase [*Mmp13*$^{-/-}$, 0.295±0.026 (n=4); wild type, 0.069±0.022 (n=3), as total bone volume per tissue volume (mean±s.e.m., P=0.0015, two-tailed t-test)] in trabecular bone volume in the *Mmp13*$^{-/-}$ mice compared with wild-type littermates (Fig. 3I,J). Interestingly, the cortical bone volume was not significantly different. By one year of age, the trabecular volume in *Mmp13*$^{-/-}$ was comparable with wild type (data not shown). These data suggest that a role for *Mmp13* is confined to the most active stages of trabecular bone remodeling.

Chondrocyte differentiation is normal but growth plate exit is delayed in *Mmp13*$^{-/-}$ mice

The observed increase in the hypertrophic chondrocyte zone of *Mmp13*$^{-/-}$ growth plates could be the result of increased cell proliferation, altered differentiation or a reduced rate of

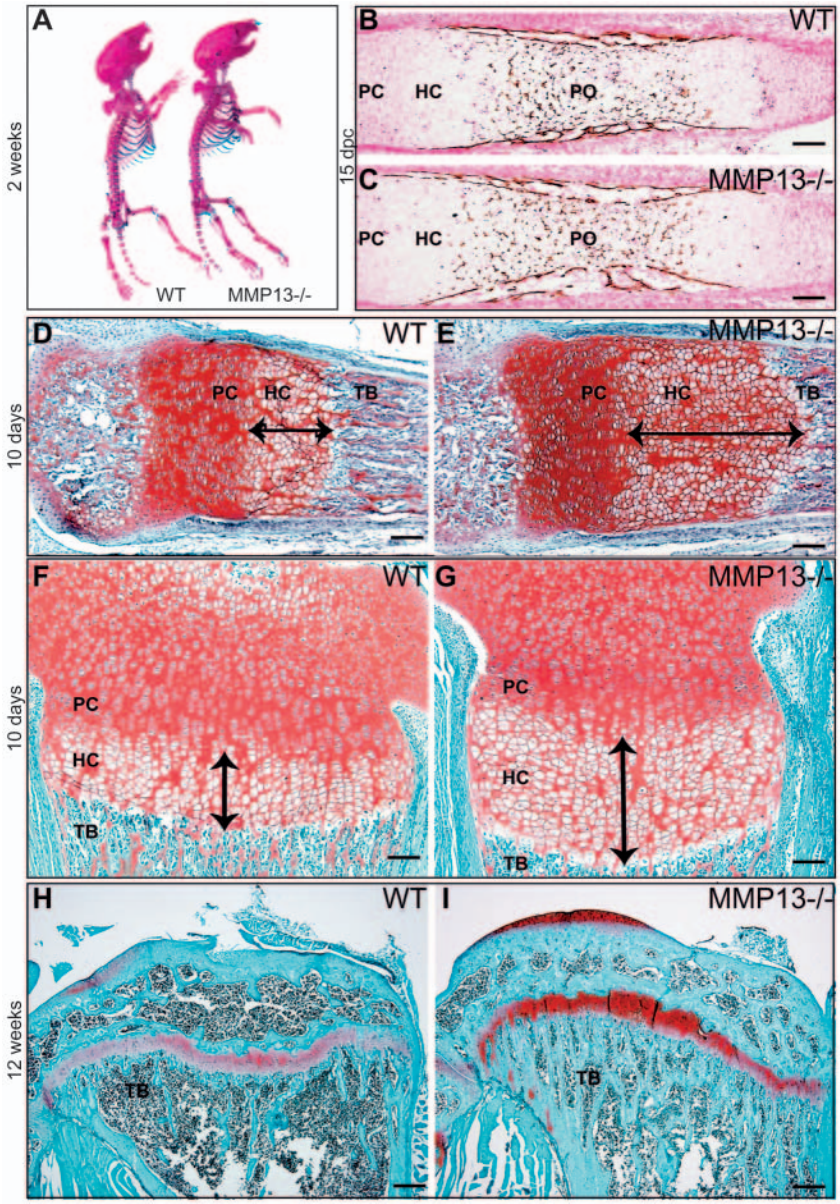

Fig. 2. Histological examination of the *Mmp13*$^{-/-}$ growth plate defect. (A) Alizarin Red/Alcian Blue staining of whole skeletons from 2-week-old wild-type and *Mmp13*$^{-/-}$ mice showing no overt difference in overall skeletal structure between genotypes. (B,C) Von Kossa stained tibia from 15 dpc wild-type and *Mmp13*$^{-/-}$ mice shows the presence of mineralized tissue in the diaphyses of both genotypes. No overt difference is evident in proliferating chondrocyte (PC) zones, hypertrophic chondrocyte (HC) zones or primary ossification centers (PO) between genotypes. (D,E) Safranin-O stained metatarsals from 10-day-old wild-type and *Mmp13*$^{-/-}$ mice; (F,G) Safranin-O stained tibia from 10-day-old wild-type and *Mmp13*$^{-/-}$ mice. *Mmp13*$^{-/-}$ mice have an expansion of the hypertrophic chondrocyte (HC) zone of the growth plates of (compare lengths indicated by black bars). (H,I) Safranin-O stained tibia from 12-week-old wild-type and *Mmp13*$^{-/-}$ mice. The expansion of the hypertrophic cartilage is ameliorated but Safranin-O staining remains more intense in the mutant growth plate (TB, trabecular bone). Scale bars: 100 μm in B-G; 200 μm in H,I.

programmed cell death of hypertrophic chondrocytes in the growth plate. To assess chondrocyte proliferation, we labeled mice with bromodeoxyuridine (BrdU) (Vu et al., 1998). Tibiae harvested from one-week-old BrdU-labeled *Mmp13*$^{-/-}$ and wild-type mice showed a similar number of labeled cells in the proliferating zone of the growth plate (Fig. 4A). Thus, the expansion of the zone of hypertrophic cartilage is not the result of increased chondrocyte proliferation.

We then examined chondrocyte differentiation using several stage-specific differentiation markers. Col2 (encoded by *Col2A1 and Col2A2*) is expressed by resting and proliferating chondrocytes. In situ hybridization using a probe to murine *Col2A1* showed no difference in the Col2 expression pattern in growth plates of *Mmp13*$^{-/-}$ mice when compared with wild-type littermates (Fig. 4B). Using a *Col10A1* probe, we found that collagen type X, which is expressed by hypertrophic chondrocytes, showed an expanded expression domain corresponding to the increased hypertrophic zone. Vascular endothelial growth factor (*VEGF*) is a marker for the most terminal rows of late hypertrophic chondrocytes (Gerber et al., 1999). In the growth plate of *Mmp13*$^{-/-}$ mice, the expression domain of *Vegf* increased considerably. Osteopontin (*Osp*), which is expressed in the very last row of terminally differentiated hypertrophic chondrocytes and in osteoblasts, expanded in expression in the hypertrophic chondrocyte zone of the growth plate of *Mmp13*$^{-/-}$ mice (Fig. 4). Taken together, these results suggest that in the endochondral bones of *Mmp13*$^{-/-}$ mice, chondrocytes proliferate and differentiate normally, but accumulate in the most terminally differentiated hypertrophic state as their exit from the growth plate is delayed.

Mice with conditional deletion of *Mmp13* have specific hypertrophic cartilage and trabecular bone phenotypes

The increased trabecular bone density observed in the *Mmp13*$^{-/-}$ mice could be the consequence of improper cartilage matrix degradation caused by MMP13 deficiency in late hypertrophic chondrocytes. Alternatively, a defect in trabecular bone formation could be the result of the MMP13 deficiency in osteoblasts. To test which of these mechanisms is responsible for the trabecular bone defects, we conditionally inactivated *Mmp13* in chondrocytes or osteoblasts. For this purpose, we crossed floxed *Mmp13* mice (MMP13fl/fl) to mice carrying the Cre recombinase transgene under control of the *Col2A1* promoter (Col2-Cre) or by the *Col1α1* promoter (Col1-Cre). MMP13+/fl;Col2-Cre$^{+/-}$ or MMP13+/fl;Col1-Cre$^{+/-}$ mice were then crossed to MMP13fl/fl mice.

As expected, MMP13fl/fl;Col2-Cre$^{+/-}$ mice displayed a similar increase in hypertrophic chondrocytes as observed in

Mmp13$^{-/-}$ mice (Fig. 5A,B). In contrast to *Mmp13*$^{-/-}$ mice, MMP13fl/fl;Col2-Cre$^{+/-}$ mice did not show a noticeable increase in trabecular bone volume (Fig. 5C,D). However, we noted that the spicules of trabecular bone in MMP13fl/fl;Col2-Cre$^{+/-}$ were irregular in shape and length when compared with wild-type mice. This is similar to the irregular organization of trabecular bone seen initially in the *Mmp13*$^{-/-}$ mice (Fig. 3), and suggests that ablation of MMP13 from chondrocytes has only a mild modeling affect on trabecular bone. The absence of an overt change in trabecular bone in MMP13fl/fl;Col2-Cre$^{+/-}$ mice indicates that the increased trabecular bone

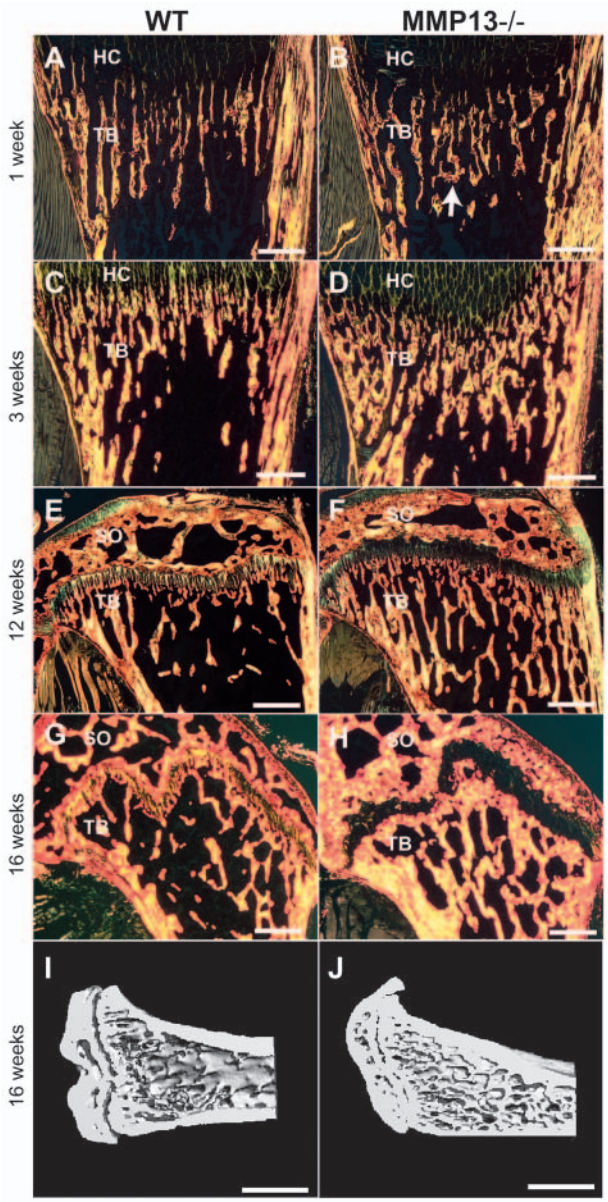

Fig. 3. Histological examination of the *Mmp13*$^{-/-}$ trabecular bone defect. (A,B) Picrosirius Red stained tibia from 1-week-old mice show no apparent increase in trabecular bone (TB) in *Mmp13*$^{-/-}$ mice compared with wild type, but the bone spicules in *Mmp13*$^{-/-}$ mice are irregular in shape (indicated by arrow). At 3 weeks of age, *Mmp13*$^{-/-}$ mice show increased trabecular bone (C,D). Unlike the increase of hypertrophic cartilage (HC), which resolves at 5 weeks of age, the increase in trabecular bone in *Mmp13*$^{-/-}$ mice persists for months (E,F). Similar increases in trabecular bone can also be observed in femurs (G,H). Histological observations were confirmed by Micro-CT analyses on tibia of 16-week-old wild-type and *Mmp13*$^{-/-}$ mice (I,J). SO, secondary site of ossification. Scale bars: 200 μm in A,B; 300 μm in C,D; 400 μm in E-H; 1 mm in I,J.

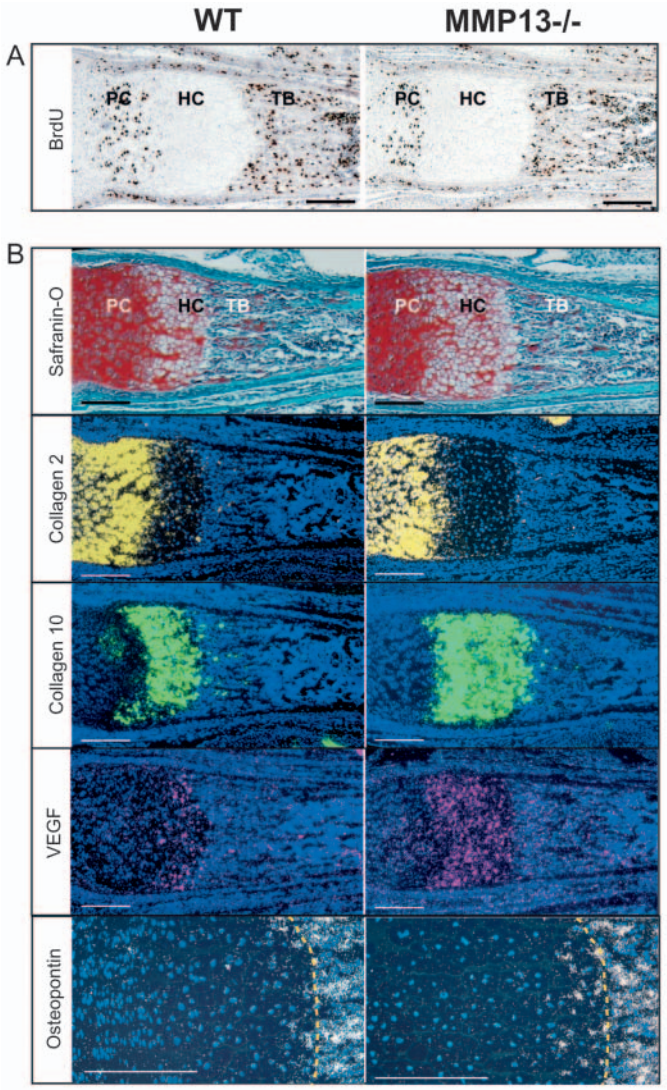

Fig. 4. Examination of differentiation markers in *Mmp13*$^{-/-}$ endochondral cartilage. (A) BrdU incorporation in 1-week-old tibia of wild-type and *Mmp13*$^{-/-}$ mice. Animals were injected with 1 μg BrdU/g mouse 1 hour prior to sacrifice. A similar number of BrdU-positive cells (brown staining) can be observed in the proliferating chondrocyte (PC) zone, and in cells within the trabecular bone (TB) for wild-type and *Mmp13*$^{-/-}$ bones, indicating that proliferation is not impaired in *Mmp13*$^{-/-}$ mice. (B) In situ hybridization on 1-week-old metatarsals with probes to chondrocyte differentiation markers show normal expression domain of col2, but expanded expression of collagen type X and VEGF, indicating an increased late hypertrophic chondrocyte population in the *Mmp13*$^{-/-}$ growth plate. In wild-type mice, expression of osteopontin (*Osp*) is restricted to only one row of hypertrophic chondrocytes in the growth plate of wild-type mice. The growth plate of *Mmp13* $^{-/-}$ mice contains several rows of chondrocytes expressing *Osp* (broken line demarcates front of ossification). Safranin-O staining shows general morphology (HC, hypertrophic cartilage). Scale bars: 100 μm.

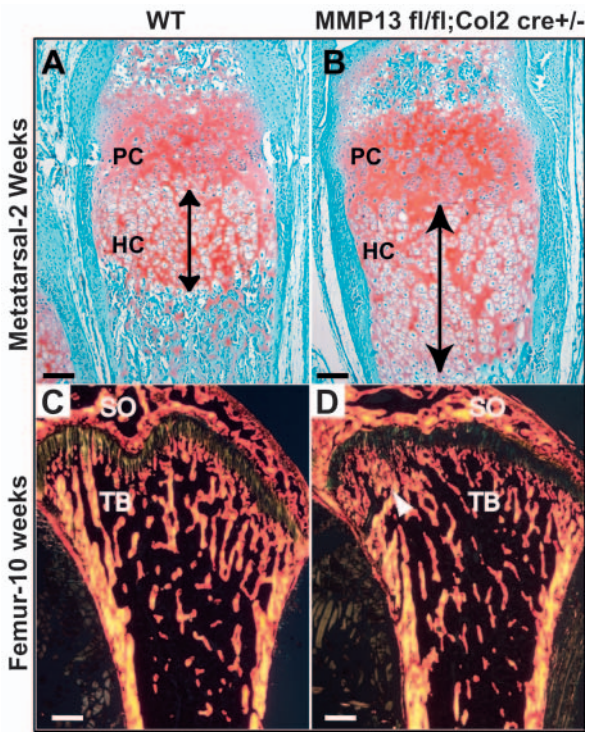

Fig. 5. Phenotype of MMP13fl/fl;Col2-Cre$^{+/-}$ endochondral bones. (A,B) Safranin-O stained metatarsals from 2-week-old wild-type and MMP13fl/fl;Col2-Cre$^{+/-}$ mice show an increased hypertrophic chondrocyte (HC) zone in MMP13fl/fl;Col2-Cre$^{+/-}$ mice similar to that observed in *Mmp13*$^{-/-}$ mice (compare with Fig. 1D,E). (C,D) Picrosirius red-stained femurs from 10-week-old wild-type and MMP13fl/fl;Col2-Cre$^{+/-}$. MMP13fl/fl;Col2-Cre$^{+/-}$ mice lack the increased trabecular bone (TB) phenotype observed in the *Mmp13*$^{-/-}$ mice, but have an altered structure of the trabeculae (arrow). SO, secondary site of ossification. Scale bars: 100 μm in A,B; 300 μm in C,D.

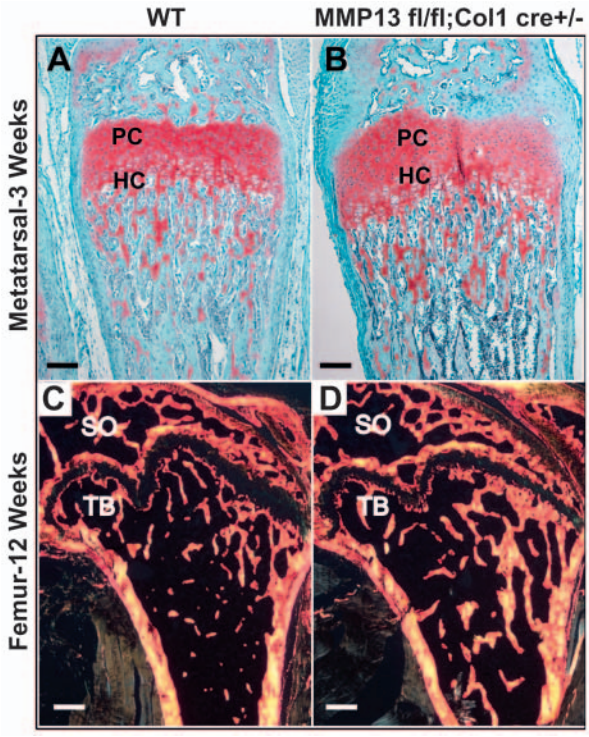

Fig. 6. Phenotype of MMP13fl/fl;Col1-Cre$^{+/-}$ endochondral bones. (A,B) Safranin-O stained metatarsals from 3-week-old wild-type and MMP13fl/fl;Col1-Cre$^{+/-}$ mice show no increase in the hypertrophic chondrocyte (HC) zone of MMP13fl/fl;Col1-Cre$^{+/-}$ mice compared with wild type. (C,D) Picrosirius Red stained femurs from 12-week-old wild-type and MMP13fl/fl;Col1-Cre$^{+/-}$. MMP13fl/fl;Col1-Cre$^{+/-}$ mice have increased trabecular bone (TB) similar to that observed in the *Mmp13*$^{-/-}$ mice (SO, secondary site of ossification. Scale bars: 100 μm in A,B; 300 μm in C,D.

observed in *Mmp13*$^{-/-}$ mice is the result of absence of *Mmp13* expression in osteoblasts.

In keeping with these observations, we predicted that conditional inactivation of MMP13 in osteoblasts would retain proper cartilage matrix remodeling, and thus would lack the increase in hypertrophic cartilage and the altered bone spicule structure. Indeed, our analysis of the MMP13+/fl;Col1-Cre$^{+/-}$, which are deficient in MMP13 in bone only, revealed a normal zone of hypertrophic cartilage but an increase in trabecular bone volume (Fig. 6).

Mmp13$^{-/-}$ mice have normal angiogenesis

Initial vascular invasion and establishment of the primary ossification center was normal in *Mmp13*$^{-/-}$ mice. In addition, there was no apparent overall difference in cell proliferation in the osteoblastic zone of wild-type and *Mmp13*$^{-/-}$ trabecular bones (Fig. 4A). Mineralization was also normal, as was bone marrow cavity formation (Fig. 7A-D). The osteoclast population, determined by tartrate-resistant acid phosphatase (TRAP) activity, a marker of differentiated osteoclasts, was also unchanged (Fig. 7A and B).

Impaired vascularization is often observed in conjunction with endochondral growth plate and trabecular bone phenotypes. However, the higher expression of VEGF in the mutant growth plates (Fig. 4B), coupled with the lack of a delay in initial vascularization (Fig. 2B,C), suggests that angiogenesis factors are unlikely to be limiting in the *Mmp13*$^{-/-}$ mice. When we immunostained 1-week-old tibiae with an antibody to platelet endothelial cell adhesion molecule (PECAM; CD31), a marker of endothelial cells, we observed no overt differences in number, localization or morphology of blood vessels in the trabecular bone of *Mmp13*$^{-/-}$ mice when compared with wild type (Fig. 7E,F). These data suggest that angiogenesis is not impaired in the mutant mice and therefore is unlikely to be the rate-limiting step for the observed endochondral phenotypes.

Mmp9$^{-/-}$; *Mmp13*$^{-/-}$ mice display a dramatic alteration in growth plate architecture and skeletal development

MMP13 is able to perform the initial fibrillar collagen cleavage and MMP9 can then degrade the denatured collagen cleavage fragments. To test the possible synergy between MMP9 and MMP13, we crossed *Mmp13*$^{-/-}$ and *Mmp9*$^{-/-}$ mice (Vu et al., 1998) to obtain animals that were deficient for both proteinases (*Mmp9*$^{-/-}$;*Mmp13*$^{-/-}$). *Mmp9*$^{-/-}$;*Mmp13*$^{-/-}$ mice were viable, but were visibly runted. The long bones of postnatal *Mmp9*$^{-/-}$;*Mmp13*$^{-/-}$ mice exhibited a dramatic phenotype in the growth plate, namely an expanded hypertrophic chondrocyte

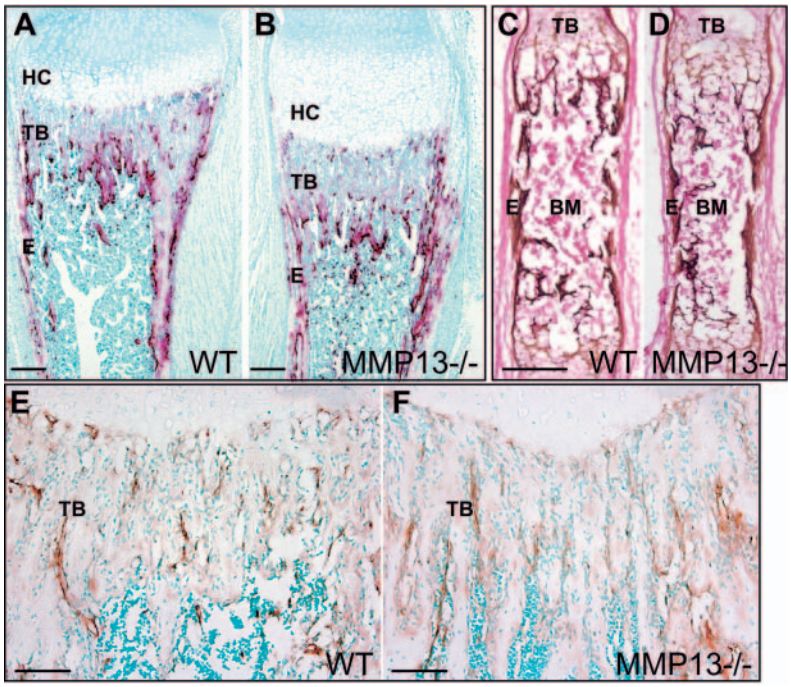

Fig. 7. Examination of key cell types in *Mmp13*$^{-/-}$ endochondral bones. (A,B) TRAP (red) stained 1-week-old wild-type and *Mmp13*$^{-/-}$ tibial epiphyses shows no difference in the osteoclast population (red staining) in the trabecular bone (TB) and endostea (E) of wild-type and *Mmp13*$^{-/-}$ mice. (C,D) Formation of the bone marrow cavity and mineralization were analyzed by Van Kossa stain on newborn wild-type and *Mmp13*$^{-/-}$ metatarsals. Mineralized tissue (brown staining) is present in endosteum (E) surrounding the bone marrow cavity, and in the surrounding trabecular bone (TB) in both wild-type and *Mmp13*$^{-/-}$ bones. (E,F) PECAM-immunostained 1-week-old tibia showing vessels (brown staining) in the trabecular bone (TB). There is no overt difference in localization or morphology of blood vessels in *Mmp13*$^{-/-}$ mice compared with wild type. Scale bars: 200 μm in A,B; 100 μm in C-F.

zone, that was more severe than the growth plate phenotype of either the *Mmp9*$^{-/-}$ or the *Mmp13*$^{-/-}$ mice. The normal columnar architecture was lost in the overpopulated *Mmp9*$^{-/-}$;*Mmp13*$^{-/-}$ hypertrophic zone, while the front of ossification took on a conformation similar to, but more severe than, that observed in the *Mmp9*$^{-/-}$ mice (Fig. 8A). mRNA in situ analyses using an *Osp*-specific probe showed an increase in the number of terminally differentiated hypertrophic cells in the MMP9/MMP13 knockout mice. This shows that exit from the growth plate is delayed, but also that the cells are viable and not necrotic (data not shown). In addition to the phenotype observed at the primary site of ossification, development of the secondary site of ossification was delayed in *Mmp9*$^{-/-}$;*Mmp13*$^{-/-}$ bones. This delay was first visible at 2 weeks of age and persisted throughout the rapid growth phase (Fig. 8A, insets). Examination of 5-month-old *Mmp9*$^{-/-}$;*Mmp13*$^{-/-}$ mice revealed that the growth plates in metatarsals did eventually close and developed secondary sites of ossification, although the structure of the residual endosteum and bone marrow cavity was slightly altered from wild type (Fig. 7B) and the mice had dramatically shortened skeletal elements (Fig. 8C).

Unlike the *Mmp13*$^{-/-}$ mice, which have increased trabecular bone volume, the *Mmp9*$^{-/-}$ mice have decreased trabecular bone volume. However, the amount of trabecular bone made in the *Mmp9*$^{-/-}$;*Mmp13*$^{-/-}$ animals was clearly reduced when compared with wild-type, *Mmp9*$^{-/-}$ or *Mmp13*$^{-/-}$ mice, and the development of the bone marrow cavity was delayed (Fig. 8A). Taken together, these data indicate a strong synergy between MMP13 and MMP9 in both primary and secondary ossification centers during endochondral bone development, as well as cooperation in trabecular bone formation. This suggests that specific cleavage of ECM substrates by MMP9 and MMP13 may be crucial for proper endochondral ossification.

MMP9 and MMP13 contribute to ECM remodeling in endochondral bone formation

Our data have shown that chondrocyte proliferation, differentiation, chondrocyte apoptosis, angiogenesis and bone deposition are not rate limiting during endochondral bone formation in the *Mmp13*$^{-/-}$ mice. However, accumulation of cartilage matrix caused by expansion of the hypertrophic zone and increased trabecular bone mass are robust features of the phenotype. MMP9 and MMP13 are able to cleave aggrecan and collagen, the most abundant molecules in the developing bones, at least in vitro (Billinghurst et al., 1997; Fosang et al., 1996; Mercuri et al., 2000; Mitchell et al., 1996; Vu et al., 1998). This points to ECM remodeling as a crucial event. Accordingly, we asked whether cleavage of these two potential targets of MMP9 and/or MMP13 in the developing growth plate and trabecular bone is altered during endochondral ossification in mice deficient for MMP13 or MMP9, or both. We first used an antibody directed toward DIPEN, a cryptic epitope in aggrecan that is exposed specifically upon MMP cleavage (Singer et al., 1995) to assess the state of aggrecan degradation. This MMP-specific aggrecan cleavage epitope was present along the front of ossification in wild-type, *Mmp9*$^{-/-}$ and *Mmp13*$^{-/-}$ tibiae, but not in *Mmp9*$^{-/-}$; *Mmp13*$^{-/-}$ tibiae (Fig. 9A). In all cases, this neoepitope was confined to the last transverse septa of the growth plate (LTS). These results indicate that MMP13 and MMP9 together are responsible for MMP-dependent aggrecan cleavage.

We then used an antibody that detects a neoepitope at the cleavage site on the 3/4 fragment of Col1 and Col2 (Billinghurst et al., 1997) to assess the state of collagen remodeling. High sequence similarity between the 3/4 fragments of Col1 and Col2 allows the antibody to recognize the cleavage products of both collagens. In wild-type tibiae, cleaved collagens were present within the LTS, and were also detected along the spicules of trabecular bone (Fig. 9B). In the *Mmp13*$^{-/-}$ tibiae, cleaved collagens were absent from LTS, but were present only along the spicules of trabecular bone. By contrast, in *Mmp9*$^{-/-}$ tibiae, cleaved collagen epitopes were present only in the LTS and were absent from the trabeculae, pointing to the role of MMP13 in cartilage collagen cleavage. This suggests that MMP13 is the dominant collagenase in cartilage, but that other MMPs, most probably MMP14, contribute to collagen turnover in bone. In addition, the more

diffuse zone of cleaved collagen accumulation observed in *Mmp9*$^{-/-}$ tibiae when compared with wild type suggests that MMP9 is involved in clearing these collagen fragments after cleavage by MMP13. Surprisingly, there was less cleaved collagen present along the spicules of trabecular bone in the *Mmp9*$^{-/-}$ tibiae. This may reflect the marked delay in osteoblast recruitment and trabecular bone formation in *Mmp9*$^{-/-}$ mice (Colnot et al., 2003). In *Mmp9*$^{-/-}$;*Mmp13*$^{-/-}$ tibiae, cleaved collagens were absent from the LTS, but we did observe the neoepitope around a few chondrocytes throughout the hypertrophic zone matrix. The long persistence of the hypertrophic chondrocytes and their matrix in the *Mmp9*$^{-/-}$;*Mmp13*$^{-/-}$ mice presents an opportunity for additional proteinases that may be present only at very low levels and slowly remodel cartilage collagen in a stochastic manner. Similarly, cleaved collagen epitopes were detected at random in the small amount of bone that finally formed in the tibiae of *Mmp9*$^{-/-}$;*Mmp13*$^{-/-}$ mice, indicating that other collagenolytic proteinases can slowly compensate. The persistence of the fragments in the double nulls may be due to the lack of clearance of the cleaved fragments by MMP9. These results suggest that MMP9 and MMP13 cooperate in collagen cleavage in different regions of the developing long bones.

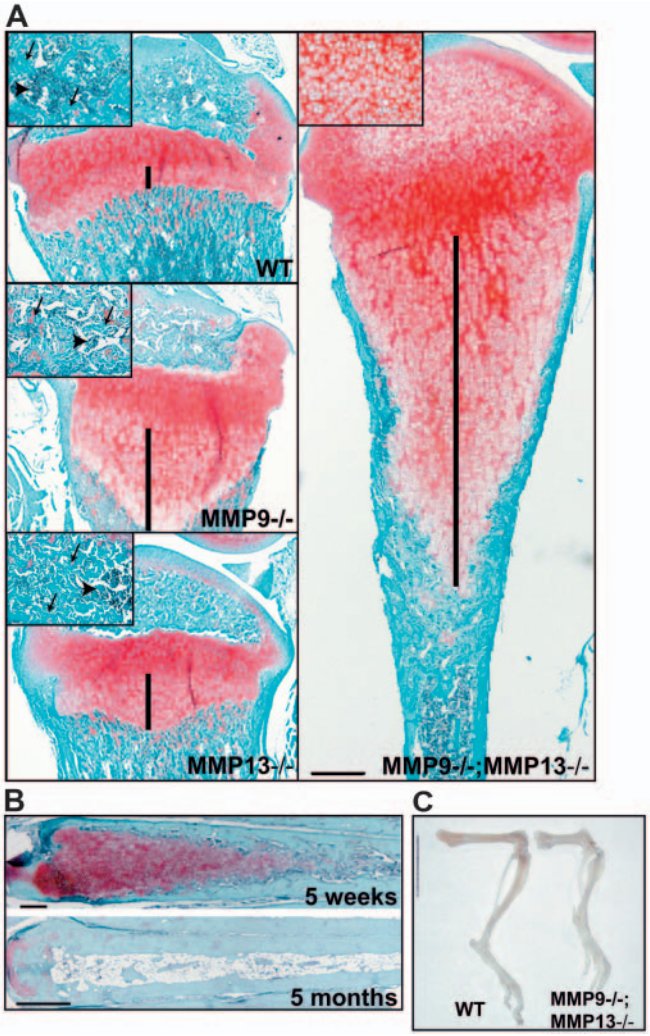

Fig. 8. Examination of *Mmp9*$^{-/-}$, *Mmp13*$^{-/-}$ and *Mmp9*$^{-/-}$;*Mmp13*$^{-/-}$ endochondral bones. (A) Safranin-O staining of 2-week-old tibiae of wild-type, *Mmp9*$^{-/-}$, *Mmp13*$^{-/-}$ and *Mmp9*$^{-/-}$;*Mmp13*$^{-/-}$ mice. *Mmp9*$^{-/-}$ and *Mmp13*$^{-/-}$ tibiae have increased zones of hypertrophic cartilage, but a dramatically expanded hypertrophic chondrocyte zone can be observed in *Mmp9*$^{-/-}$;*Mmp13*$^{-/-}$ tibia (compare lengths indicated by black bars). Magnifications of secondary ossification sites (insets) of Safranin-O stained 2-week-old tibia of wild type, *Mmp9*$^{-/-}$, *Mmp13*$^{-/-}$ and *Mmp9*$^{-/-}$;*Mmp13*$^{-/-}$ mice demonstrate delay in initiation of ossification at the secondary site in *Mmp9*$^{-/-}$;*Mmp13*$^{-/-}$. Collagenous bone tissue and colonizing blood cells in wild-type, *Mmp9*$^{-/-}$ and *Mmp13*$^{-/-}$ secondary sites are indicated by arrows and arrowheads, respectively. (B) Safranin-O staining of 5-week-old and 5-month-old metatarsals from *Mmp9*$^{-/-}$;*Mmp13*$^{-/-}$ mice showing that while 5-week-old *Mmp9*$^{-/-}$;*Mmp13*$^{-/-}$ metatarsals still display the expanded hypertrophic chondrocyte zone characteristic of this genotype, 5-month-old *Mmp9*$^{-/-}$;*Mmp13*$^{-/-}$ metatarsals display a closed growth plate, indicating recovery. (C) Whole skeletal preparations of hind limbs from 12-month-old wild-type and *Mmp9*$^{-/-}$;*Mmp13*$^{-/-}$ mice shows a shortening of all elements of the *Mmp9*$^{-/-}$;*Mmp13*$^{-/-}$ hind limb when compared with wild type. Scale bars: 300 μm in A; 200 μm in B.

Discussion

During endochondral ossification, chondrocyte differentiation and bone formation are tightly coupled in a process that involves chondrocyte apoptosis, cartilage matrix remodeling, vascular invasion and trabecular bone formation (Karsenty and Wagner, 2002; Ortega et al., 2004). How this process is controlled, and which of these steps is rate limiting has remained unclear. Although hypertrophic chondrocyte death may precede ECM degradation, previous studies show that mice with a null mutation in the gene for anti-apoptotic protein galectin 3 accumulate empty lacuna at the junction between avascular cartilage and vascular bone, without an acceleration of endochondral ossification (Colnot et al., 2001). Thus, chondrocyte apoptosis can be uncoupled from ECM remodeling and vascularization. Our data exploiting *Mmp13*$^{-/-}$, *Mmp9*$^{-/-}$ and *Mmp9*$^{-/-}$;*Mmp13*$^{-/-}$ mice point to remodeling of the cartilage matrix as the rate-limiting step in endochondral ossification.

Cartilage degradation depends on degradation of its most abundant ECM component, fibrillar collagen (Alini et al., 1992; Mwale et al., 2000), which can be cleaved by collagenolytic MMPs (Sternlicht and Werb, 2001; Werb, 1997). In this study we have demonstrated, for the first time in vivo, a specific role for MMP13 in the processes of endochondral ossification. Our data, together with the observations made in MMP14 (MT1-*Mmp*)$^{-/-}$ mice (Holmbeck et al., 1999), indicate that MMP13 is the major collagenase for Col2 cleavage. In the face of continued VEGF expression in the expanded hypertrophic cartilage zone of *Mmp13*$^{-/-}$ mice, it is apparent that degradation of Col2 may be required for vascular invasion, even in the presence of abundant angiogenic stimuli. An interesting recent study demonstrates that migration of endothelial cells and vessel formation can be prevented or substantially diminished when a mutant type I collagen that is resistant to cleavage by MMPs is used as the matrix for the explants (Zijlstra et al., 2004). In our study, the ablation of *Mmp13* did not affect blood vessel morphology at the bone-cartilage junction. However, to maintain the normal appearance of the blood vessels without an accumulation of endothelial cells in the *Mmp13*$^{-/-}$ growth plate, it follows that

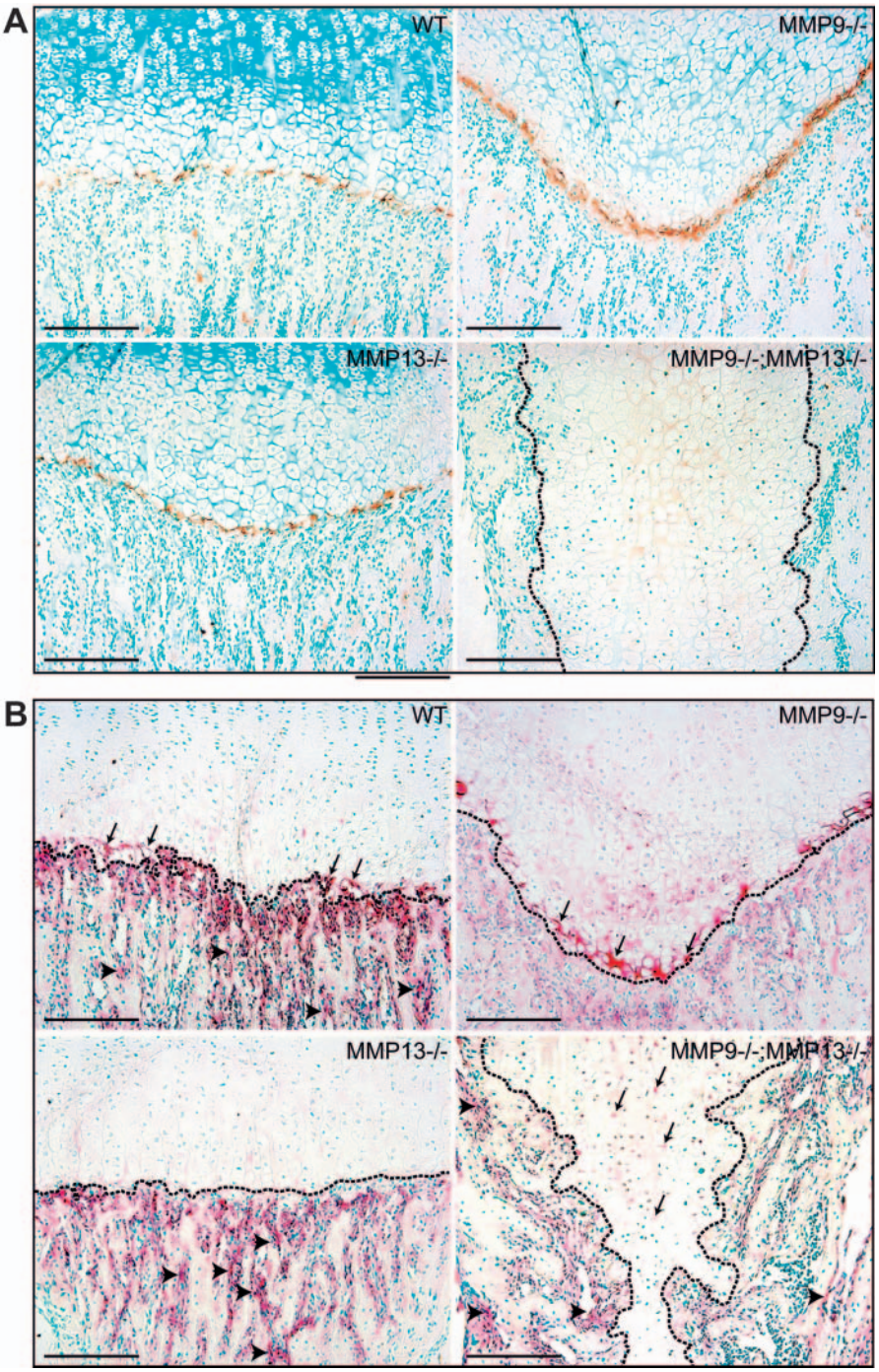

Fig. 9. Altered ECM remodeling in *Mmp9*$^{-/-}$, *Mmp13*$^{-/-}$ and *Mmp9*$^{-/-}$;*Mmp13*$^{-/-}$ long bones. (A) Immunostaining of 2-week-old tibia of wild-type, *Mmp9*$^{-/-}$, *Mmp13*$^{-/-}$ and *Mmp9*$^{-/-}$;*Mmp13*$^{-/-}$ mice with an antibody to the DIPEN neoepitope of *Mmp*-cleaved aggrecan. Cleaved aggrecan (brown staining) is present along the primary front of ossification in wild-type, *Mmp9*$^{-/-}$ and *Mmp13*$^{-/-}$ bones, no positive staining is apparent in *Mmp9*$^{-/-}$;*Mmp13*$^{-/-}$ bones. (B) Immunostaining of 2-week-old tibia of wild-type, *Mmp9*$^{-/-}$, *Mmp13*$^{-/-}$ and *Mmp9*$^{-/-}$;*Mmp13*$^{-/-}$ mice with an antibody to the 3/4 cleavage fragment of col1 and col2. The primary front of ossification (indicated by a broken line) shows the presence of cleaved collagen (pink staining) in transverse septa surrounding the most terminal hypertrophic chondrocytes (arrows) in wild-type and *Mmp9*$^{-/-}$ bones, along the trabeculae of the developing trabecular bone (arrowheads) in wild-type and *Mmp13*$^{-/-}$ bones, and at random throughout the hypertrophic chondrocyte zone (arrows) and trabecular bone (arrowheads) in *Mmp9*$^{-/-}$;*Mmp13*$^{-/-}$ bones. Scale bars: 200 μm in A; 100 μm in B.

the vascular development would have to be diminished in proportion to the increased persistence of the hypertrophic cartilage. A logical extension of this hypothesis is that increasing levels of MMP13 should accelerate vascularization, which it does (Zijlstra et al., 2004). Taken together, these observations place MMP13 upstream of angiogenesis and suggest that degradation of the cartilage ECM creates a permissive environment for blood vessels to invade.

What are the critical events on the cartilage side?

As MMP13 is the dominant collagenase in cartilage, it is not surprising that its absence caused a delay in endochondral ossification. At the cartilage-bone interface, only a thin layer of cartilage matrix separates the hypertrophic chondrocytes from invading capillaries. This layer is known as the last transverse septa (LTS) (Lee et al., 1999). The LTS is an active site of matrix remodeling, marked by degradation of fibrillar collagen. Our studies have shown that MMP13 is the major collagenase involved in degradation of Col2 at this site. The region of Col2 cleavage is restricted to the LTS, while MMP13 is expressed in a slightly larger area of the hypertrophic chondrocyte zone. As MMP13 is secreted in a latent form, it is possible that its activation occurs only at the LTS, proximal to the expression domain of its major activator MMP14 (Jimenez et al., 2001; Knauper et al., 1996).

The other major component of the cartilage matrix is aggrecan. Recent studies have shown that aggrecan protects cartilage collagen from degradation by proteinases, including MMPs (Pratta et al., 2003), and that there is an inverse relationship between collagenolytic activity and glycosaminoglycan content in hypertrophic cartilage (Byers et al., 1997; Mwale et al., 2000). This suggests that for collagenases to cleave fibrillar collagens effectively, aggrecan would first have to be degraded in this environment. This is interesting to consider, as our studies show that MMP13 and MMP9 synergize to cleave aggrecan and Col2 in the most terminal hypertrophic zone of the growth plate. Thus, it is possible that MMP9 and/or MMP13 are first responsible for clearing aggrecan molecules in this microenvironment, and that this degradation is then followed by cleavage of Col2 by MMP13.

What are the critical events on the bone side?

In addition to the expansion of the hypertrophic zone, long bones of *Mmp13*$^{-/-}$ mice have increased trabecular bone. In contrast to the expansion of the hypertrophic cartilage observed in these animals, the increase in trabecular bone persists for months. Conditional inactivation of *Mmp13* in chondrocytes shows that the increased trabecular bone mass observed in *Mmp13*$^{-/-}$ mice occurs independently of the reduced cartilage ECM degradation caused by loss of this proteinase in late hypertrophic chondrocytes. The absence of MMP13 does not abolish collagen degradation in the trabeculae, but it is unlikely that this is due to a compensatory mechanism of upregulation of other MMPs that cleave collagen, as no change in expression levels of other MMPs present in bone and cartilage was observed (see Fig. S1 in the supplementary material). We favor a scenario in which other MMPs that generally play minor roles in this area, most probably MMP14, compensate sufficiently to allow endochondral ossification to proceed. Interestingly, cortical bone is unaffected by the lack of MMP13, suggesting other MMPs contribute to its remodeling.

Formation of trabecular bone involves modeling as well as remodeling processes, and it appears that MMP13 is involved in both. Initially, *Mmp13*$^{-/-}$ mice do not display increased trabecular bone volume, but the spicules are irregular in shape. An increase in trabecular bone becomes apparent when mice reach 3 weeks of age, peaks at about 6 months of age and then gradually normalizes. By contrast, conditional inactivation of *Mmp13* in cartilage leads to irregularities in trabecular bone spicules similar to those seen in *Mmp13*$^{-/-}$ mice early in development. It is not surprising that a defect in cartilage matrix remodeling would affect trabecular bone formation, as trabecular bone is laid down upon the remnants of calcified cartilage. Upon vascularization of the hypertrophic cartilage, osteoprogenitor cells reach the interior of this zone and differentiate on the plates of mineralized cartilage between the columns of hypertrophic chondrocytes (Maes et al., 2002). Therefore, it is possible that osteoblast differentiation and function depends on the correct remodeling of cartilage, and that the altered residual cartilage matrix in *Mmp13*$^{-/-}$ endochondral bones causes impaired osteoblast differentiation and subsequent improper bone deposition (Maes et al., 2002). In keeping with these observations, conditional inactivation of MMP13 in osteoblasts maintained proper hypertrophic cartilage remodeling, but showed increased trabecular bone. Thus, the action of MMP13 in cartilage contributes to modeling of trabecular bone, while the action of MMP13 in osteoblasts contributes to remodeling of trabecular bone.

It is important to note that the *Mmp13*$^{-/-}$ bone phenotype is not the same as that produced by altering the susceptibility of the collagen substrate. Mice with targeted mutations in *Col1α1* that render Col1 collagenase-resistant show increased bone deposition (Zhao et al., 2000). However, the resistant collagen phenotype is late and occurs mainly in the cortical bone, unlike the early trabecular bone phenotype of the *Mmp13*$^{-/-}$ mice. Second, mice with collagenase-resistant Col1 have increased apoptosis of osteocytes (Zhao et al., 2000), lending further support to the evidence that collagen cleavage products may be anti-apoptotic (Montgomery et al., 1994). We did not observe increased apoptosis in the *Mmp13*$^{-/-}$ mice, as other MMPs expressed in bone and cartilage (Sasano et al., 2002) still cleave collagens at low rates in *Mmp13*$^{-/-}$ mice, and this may be sufficient to prolong cell survival and prevent accumulation of cortical bone with age in these mice.

Synergy between MMP13 and MMP9

Our data show that MMP9 and MMP13 synergize during endochondral ossification. These MMPs may first act to degrade aggrecan in the hypertrophic zone of the growth plate, making Col2 accessible to cleavage by MMP13. MMP9 may then act downstream to clear denatured collagen cleavage products generated by MMP13. Although MMPs have not been considered to be the major aggrecanases (Arner, 2002; Malfait et al., 2002), our data suggest that they do contribute to the physiological and developmental turnover of aggrecan in this region. Our studies in mice that lack both MMP9 and MMP13 support the hypothesis that MMP9 and MMP13 act synergistically to degrade the LTS. And although cathepsins also produce degradation fragments identical to those created by MMP-mediated cleavage of aggrecan (Mort et al., 1998), our data from the *Mmp9*$^{-/-}$;*Mmp13*$^{-/-}$ mice show that these MMPs are major proteinases involved in degradation of aggrecan in the growth plate.

Double null mice have a dramatic accumulation of hypertrophic cartilage accompanied by loss of normal growth plate architecture. The bone phenotype of *Mmp9*$^{-/-}$ mice was dominant in the *Mmp9*$^{-/-}$;*Mmp13*$^{-/-}$ mice; these animals displayed less trabecular bone and delayed bone marrow cavity formation. MMP9 has important roles in osteoclast and osteoblast recruitment and function (Colnot et al., 2003), as well endothelial progenitor mobilization (Hattori et al., 2003; Heissig et al., 2003). Nevertheless, the resolution of the phenotypes that occurs after several months indicates other processes are able to compensate in the absence of MMP9 and MMP13. However, this compensation is stochastic and incomplete, as the bones that do form are shorter and misshapen when compared with wild type.

How does ECM turnover relate to angiogenesis?

Chondrocyte differentiation and bone formation are tightly coupled in a process that involves chondrocyte apoptosis, cartilage matrix remodeling and vascular invasion. A number of previous studies have focused on angiogenesis as the critical step in the process. However, chondrocyte apoptosis can be uncoupled from vascularization, as inactivation of galectin 3 leads to precocious hypertrophic chondrocyte death without an alteration in angiogenesis (Colnot et al., 2001). Removal of angiogenic stimuli by ablating VEGF from hypertrophic chondrocytes (Maes et al., 2002; Zelzer et al., 2004) or by blocking VEGF receptors (Gerber et al., 1999) results in expansion of the hypertrophic cartilage zone. Likewise, angiogenesis may be uncoupled from ECM remodeling because the process of inhibiting VEGF function also inhibits VEGF-dependent recruitment of the MMP9-expressing osteoclasts needed to promote ECM remodeling (Gerber et al., 1999). However, in both the *Mmp13*$^{-/-}$ and *Mmp9*$^{-/-}$ mice, osteoclast recruitment still occurs, but, as the ECM degradation is decreased, in parallel the vasculature recruitment keeps pace with the slower rate of endochondral ossification. These observations suggest that degradation of the cartilage ECM creates a permissive environment for blood vessels to invade. Cleaving of ECM molecules could merely create a passage

way for invading blood vessels that otherwise would not be able to penetrate the dense cartilage matrix. Alternatively, cleaving of matrix molecules could make angiogenic factors accessible. Remodeling of the cartilage matrix is likely the rate-limiting step as it depends on degradation of its most abundant component, fibrillar collagen.

Insights from human skeletal disorders

The importance of matrix components in maintaining structural integrity and function of cartilage, as well as the role of the cartilage matrix in the differentiation process of its cellular components is well known. Genetic defects in humans and targeted mutagenesis in mice have demonstrated that aberrant assembly of cartilage matrix can lead to severe impairment of endochondral ossification (for a review, see Aszodi et al., 2000). SEMD is a heterogeneous group of human skeletal disorders characterized by defective growth and modeling of the long bones, which in most cases is caused by mutations in cartilage matrix proteins such as Col2 (Borochowitz et al., 2004; Tiller et al., 1995). The Missouri variant of SEMD (Gertner et al., 1997) is caused by to a point mutation in MMP13 (Kennedy et al., 2003). As is the case in our *Mmp13*$^{-/-}$ mice, the human phenotype is developmental and is ameliorated with age. This is evidence that proper endochondral ossification requires not only assembly of cartilage collagens but also their degradation.

We are grateful to Helen Capili for her outstanding patience and skill in sectioning the many skeletal elements; Yebin Jiang for assistance with the micro-CT; Ernestina Schipani for the Col2 Cre mice; Caroline Damsky for the Col1 Cre mice; and Gail Martin for the β-actin Cre mice. This work was supported by funds from the National Institutes of Health (AR46238 and AG23218 to Z.W.) and the Deutsche Forschungsgemeinschaft (An 182/6-3 to P.A.). D.S. is a Wyeth fellow of the Life Sciences Research Foundation, B. Heyer was a Alexander von Humboldt Foundation fellow, N.O. was a fellow of the Osteogenesis Imperfecta Foundation, and D.J.B. is a University of California Regents Fellow.

Supplementary material

Supplementary material for this article is available at
http://dev.biologists.org/cgi/content/full/131/23/5883/DC1

References

Abbaszade, I., Liu, R. Q., Yang, F., Rosenfeld, S. A., Ross, O. H., Link, J. R., Ellis, D. M., Tortorella, M. D., Pratta, M. A., Hollis, J. M. et al. (1999). Cloning and characterization of ADAMTS11, an aggrecanase from the ADAMTS family. *J. Biol. Chem.* **274**, 23443-23450.

Albrecht, U., Eichele, G., Helms, J. A. and Lu, H. (1997). Visualization of gene expression patterns by in situ hybridization. In *Molecular and Cellular Methods in Developmental Toxicology* (ed. G. Daston), pp. 23-48. Boca Raton, FL: CRC Press.

Alini, M., Matsui, Y., Dodge, G. R. and Poole, A. R. (1992). The extracellular matrix of cartilage in the growth plate before and during calcification: changes in composition and degradation of type II collagen. *Calcif. Tissue Int.* **50**, 327-335.

Arner, E. C. (2002). Aggrecanase-mediated cartilage degradation. *Curr. Opin. Pharmacol.* **2**, 322-329.

Aszodi, A., Bateman, J. F., Gustafsson, E., Boot-Handford, R. and Fassler, R. (2000). Mammalian skeletogenesis and extracellular matrix: what can we learn from knockout mice? *Cell Struct. Funct.* **25**, 73-84.

Billinghurst, R. C., Dahlberg, L., Ionescu, M., Reiner, A., Bourne, R., Rorabeck, C., Mitchell, P., Hambor, J., Diekmann, O., Tschesche, H. et al. (1997). Enhanced cleavage of type II collagen by collagenases in osteoarthritic articular cartilage. *J. Clin. Invest.* **99**, 1534-1545.

Borochowitz, Z. U., Scheffer, D., Adir, V., Dagoneau, N., Munnich, A. and Cormier-Daire, V. (2004). Spondylo-epi-metaphyseal dysplasia (SEMD) matrilin 3 type: homozygote matrilin 3 mutation in a novel form of SEMD. *J. Med. Genet.* **41**, 366-372.

Byers, S., van Rooden, J. C. and Foster, B. K. (1997). Structural changes in the large proteoglycan, aggrecan, in different zones of the ovine growth plate. *Calcif. Tissue Int.* **60**, 71-78.

Colnot, C. I. and Helms, J. A. (2001). A molecular analysis of matrix remodeling and angiogenesis during long bone development. *Mech. Dev.* **100**, 245-250.

Colnot, C., Sidhu, S. S., Balmain, N. and Poirier, F. (2001). Uncoupling of chondrocyte death and vascular invasion in mouse galectin 3 null mutant bones. *Dev. Biol.* **229**, 203-214.

Colnot, C., Thompson, Z., Miclau, T., Werb, Z. and Helms, J. A. (2003). Altered fracture repair in the absence of MMP9. *Development* **130**, 4123-4133.

Dacquin, R., Starbuck, M., Schinke, T. and Karsenty, G. (2002). Mouse alpha1(I)-collagen promoter is the best known promoter to drive efficient Cre recombinase expression in osteoblast. *Dev. Dyn.* **224**, 245-251.

Doege, K. J. (1999). Aggrecan. In *Guidebook to the Extracellular Matrix, Anchor and Adhesion Proteins* (ed. V. R. Kreis), pp. 359-361. New York: Oxford University Press.

Engsig, M. T., Chen, Q. J., Vu, T. H., Pedersen, A. C., Therkidsen, B., Lund, L. R., Henriksen, K., Lenhard, T., Foged, N. T., Werb, Z. et al. (2000). Matrix metalloproteinase 9 and vascular endothelial growth factor are essential for osteoclast recruitment into developing long bones. *J. Cell Biol.* **151**, 879-889.

Fields, G. B., van Wart, H. E. and Birkedal-Hansen, H. (1987). Sequence specificity of human skin fibroblast collagenase. Evidence for the role of collagen structure in determining the collagenase cleavage site. *J. Biol. Chem.* **262**, 6221-6226.

Fosang, A. J., Last, K., Knauper, V., Murphy, G. and Neame, P. J. (1996). Degradation of cartilage aggrecan by collagenase-3 (MMP-13). *FEBS Lett.* **380**, 17-20.

Gack, S., Vallon, R., Schmidt, J., Grigoriadis, A., Tuckermann, J., Schenkel, J., Weiher, H., Wagner, E. F. and Angel, P. (1995). Expression of interstitial collagenase during skeletal development of the mouse is restricted to osteoblast-like cells and hypertrophic chondrocytes. *Cell Growth Differ.* **6**, 759-767.

Gerber, H. P., Vu, T. H., Ryan, A. M., Kowalski, J., Werb, Z. and Ferrara, N. (1999). VEGF couples hypertrophic cartilage remodeling, ossification and angiogenesis during endochondral bone formation. *Nat. Med.* **5**, 623-628.

Gertner, J. M., Whyte, M. P., Dixon, P. H., Pang, J. T., Trump, D., Pearce, S. H., Wooding, C. and Thakker, R. V. (1997). Linkage studies of a Missouri kindred with autosomal dominant spondyloepimetaphyseal dysplasia (SEMD) indicate genetic heterogeneity. *J. Bone Miner. Res.* **12**, 1204-1209.

Hattori, K., Heissig, B. and Rafii, S. (2003). The regulation of hematopoietic stem cell and progenitor mobilization by chemokine SDF-1. *Leuk Lymphoma* **44**, 575-582.

Heissig, B., Werb, Z., Rafii, S. and Hattori, K. (2003). Role of c-kit/Kit ligand signaling in regulating vasculogenesis. *Thromb. Haemost.* **90**, 570-576.

Holmbeck, K., Bianco, P., Caterina, J., Yamada, S., Kromer, M., Kuznetsov, S. A., Mankani, M., Robey, P. G., Poole, A. R., Pidoux, I. et al. (1999). MT1-MMP-deficient mice develop dwarfism, osteopenia, arthritis, and connective tissue disease due to inadequate collagen turnover. *Cell* **99**, 81-92.

Jiang, Y., Zhao, J. J., Mitlak, B. H., Wang, O., Genant, H. K. and Eriksen, E. F. (2003). Recombinant human parathyroid hormone (1-34) [teriparatide] improves both cortical and cancellous bone structure. *J. Bone Miner. Res.* **18**, 1932-1941.

Jimenez, M. J., Balbin, M., Alvarez, J., Komori, T., Bianco, P., Holmbeck, K., Birkedal-Hansen, H., Lopez, J. M. and Lopez-Otin, C. (2001). A regulatory cascade involving retinoic acid, Cbfa1, and matrix metalloproteinases is coupled to the development of a process of perichondrial invasion and osteogenic differentiation during bone formation. *J. Cell Biol.* **155**, 1333-1344.

Johansson, N., Saarialho-Kere, U., Airola, K., Herva, R., Nissinen, L., Westermarck, J., Vuorio, E., Heino, J. and Kahari, V. M. (1997). Collagenase-3 (MMP-13) is expressed by hypertrophic chondrocytes, periosteal cells, and osteoblasts during human fetal bone development. *Dev Dyn* **208**, 387-397.

Karsenty, G. and Wagner, E. F. (2002). Reaching a genetic and molecular understanding of skeletal development. *Dev. Cell* **2**, 389-406.

Kennedy, A. M., Christie, P. T., Harding, B., Pannett, A. A. J., Dearlove, A., Whyte, M. P. and Thakker, R. V. (2003). Matrix metalloproteinase 13 (MMP13) mutation causes spondyloepimetaphyseal dysplasia (SEMD), Missouri variant. *Endocr. Abstr.* **5**, OC40.

Knauper, V., Will, H., Lopez-Otin, C., Smith, B., Atkinson, S. J., Stanton, H., Hembry, R. M. and Murphy, G. (1996). Cellular mechanisms for human procollagenase-3 (MMP-13) activation. Evidence that MT1-MMP (MMP-14) and gelatinase a (MMP-2) are able to generate active enzyme. *J. Biol. Chem.* **271**, 17124-17131.

Kuno, K., Okada, Y., Kawashima, H., Nakamura, H., Miyasaka, M., Ohno, H. and Matsushima, K. (2000). ADAMTS-1 cleaves a cartilage proteoglycan, aggrecan. *FEBS Lett.* **478**, 241-245.

Lee, E. R., Murphy, G., El-Alfy, M., Davoli, M. A., Lamplugh, L., Docherty, A. J. and Leblond, C. P. (1999). Active gelatinase B is identified by histozymography in the cartilage resorption sites of developing long bones. *Dev. Dyn.* **215**, 190-205.

Liu, X., Wu, H., Byrne, M., Jeffrey, J., Krane, S. and Jaenisch, R. (1995). A targeted mutation at the known collagenase cleavage site in mouse type I collagen impairs tissue remodeling. *J. Cell Biol.* **130**, 227-237.

Maes, C., Carmeliet, P., Moermans, K., Stockmans, I., Smets, N., Collen, D., Bouillon, R. and Carmeliet, G. (2002). Impaired angiogenesis and endochondral bone formation in mice lacking the vascular endothelial growth factor isoforms VEGF164 and VEGF188. *Mech. Dev.* **111**, 61-73.

Malfait, A. M., Liu, R. Q., Ijiri, K., Komiya, S. and Tortorella, M. D. (2002). Inhibition of ADAM-TS4 and ADAM-TS5 prevents aggrecan degradation in osteoarthritic cartilage. *J. Biol. Chem.* **277**, 22201-22208.

McLeod, M. J. (1980). Differential staining of cartilage and bone in whole mouse fetuses by alcian blue and alizarin red S. *Teratology* **22**, 299-301.

Mercuri, F. A., Maciewicz, R. A., Tart, J., Last, K. and Fosang, A. J. (2000). Mutations in the interglobular domain of aggrecan alter matrix metalloproteinase and aggrecanase cleavage patterns. Evidence that matrix metalloproteinase cleavage interferes with aggrecanase activity. *J. Biol. Chem.* **275**, 33038-33045.

Mitchell, P. G., Magna, H. A., Reeves, L. M., Lopresti-Morrow, L. L., Yocum, S. A., Rosner, P. J., Geoghegan, K. F. and Hambor, J. E. (1996). Cloning, expression, and type II collagenolytic activity of matrix metalloproteinase-13 from human osteoarthritic cartilage. *J. Clin. Invest.* **97**, 761-768.

Montgomery, A. M., Mueller, B. M., Reisfeld, R. A., Taylor, S. M. and DeClerck, Y. A. (1994). Effect of tissue inhibitor of the matrix metalloproteinases-2 expression on the growth and spontaneous metastasis of a human melanoma cell line. *Cancer Res.* **54**, 5467-54673.

Mort, J. S., Magny, M. C. and Lee, E. R. (1998). Cathepsin B: an alternative protease for the generation of an aggrecan 'metalloproteinase' cleavage neoepitope. *Biochem. J.* **335**, 491-494.

Mwale, F., Billinghurst, C., Wu, W., Alini, M., Webber, C., Reiner, A., Ionescu, M., Poole, J. and Poole, A. R. (2000). Selective assembly and remodelling of collagens II and IX associated with expression of the chondrocyte hypertrophic phenotype. *Dev. Dyn.* **218**, 648-662.

Ortega, N., Behonick, D. J. and Werb, Z. (2004). Matrix remodeling during endochondral ossification. *Trends Cell Biol* **14**, 86-93.

Peeters-Joris, C., Hammani, K. and Singer, C. F. (1998). Differential regulation of MMP-13 (collagenase-3) and MMP-3 (stromelysin-1) in mouse calvariae. *Biochim. Biophys. Acta* **1405**, 14-28.

Pratta, M. A., Yao, W., Decicco, C., Tortorella, M. D., Liu, R. Q., Copeland, R. A., Magolda, R., Newton, R. C., Trzaskos, J. M. and Arner, E. C. (2003). Aggrecan protects cartilage collagen from proteolytic cleavage. *J. Biol. Chem.* **278**, 45539-45545.

Sasano, Y., Zhu, J. X., Tsubota, M., Takahashi, I., Onodera, K., Mizoguchi, I. and Kagayama, M. (2002). Gene expression of MMP8 and MMP13 during embryonic development of bone and cartilage in the rat mandible and hind limb. *J. Histochem. Cytochem.* **50**, 325-332.

Sauer, B. (1998). Inducible gene targeting in mice using the Cre/lox system. *Methods* **14**, 381-392.

Schipani, E., Ryan, H. E., Didrickson, S., Kobayashi, T., Knight, M. and Johnson, R. S. (2001). Hypoxia in cartilage: HIF-1alpha is essential for chondrocyte growth arrest and survival. *Genes Dev.* **15**, 2865-2876.

Schorpp, M., Mattei, M. G., Herr, I., Gack, S., Schaper, J. and Angel, P. (1995). Structural organization and chromosomal localization of the mouse collagenase type I gene. *Biochem. J.* **308**, 211-217.

Singer, II, Kawka, D. W., Bayne, E. K., Donatelli, S. A., Weidner, J. R., Williams, H. R., Ayala, J. M., Mumford, R. A., Lark, M. W., Glant, T. T. et al. (1995). VDIPEN, a metalloproteinase-generated neoepitope, is induced and immunolocalized in articular cartilage during inflammatory arthritis. *J. Clin. Invest.* **95**, 2178-2186.

Sternlicht, M. D. and Werb, Z. (2001). How matrix metalloproteinases regulate cell behavior. *Annu. Rev. Cell Dev. Biol.* **17**, 463-516.

Tiller, G. E., Polumbo, P. A., Weis, M. A., Bogaert, R., Lachman, R. S., Cohn, D. H., Rimoin, D. L. and Eyre, D. R. (1995). Dominant mutations in the type II collagen gene, COL2A1, produce spondyloepimetaphyseal dysplasia, Strudwick type. *Nat. Genet.* **11**, 87-89.

Tortorella, M. D., Burn, T. C., Pratta, M. A., Abbaszade, I., Hollis, J. M., Liu, R., Rosenfeld, S. A., Copeland, R. A., Decicco, C. P., Wynn, R. et al. (1999). Purification and cloning of aggrecanase-1: a member of the ADAMTS family of proteins. *Science* **284**, 1664-1666.

Vu, T. H., Shipley, J. M., Bergers, G., Berger, J. E., Helms, J. A., Hanahan, D., Shapiro, S. D., Senior, R. M. and Werb, Z. (1998). MMP-9/gelatinase B is a key regulator of growth plate angiogenesis and apoptosis of hypertrophic chondrocytes. *Cell* **93**, 411-422.

Werb, Z. (1982). *Collagens in Health and Disease*. New York: Churchill Livingstone.

Werb, Z. (1997). ECM and cell surface proteolysis: regulating cellular ecology. *Cell* **91**, 439-442.

Wu, H., Byrne, M. H., Stacey, A., Goldring, M. B., Birkhead, J. R., Jaenisch, R. and Krane, S. M. (1990). Generation of collagenase-resistant collagen by site-directed mutagenesis of murine pro alpha 1(I) collagen gene. *Proc. Natl. Acad. Sci. USA* **87**, 5888-5892.

Wu, W., Mwale, F., Tchetina, E., Kojima, T., Yasuda, T. and Poole, A. R. (2001). Cartilage matrix resorption in skeletogenesis. *Novartis Found. Symp.* **232**, 158-170.

Zelzer, E., Mamluk, R., Ferrara, N., Johnson, R. S., Schipani, E. and Olsen, B. R. (2004). VEGFA is necessary for chondrocyte survival during bone development. *Development* **131**, 2161-2171.

Zhao, W., Byrne, M. H., Boyce, B. F. and Krane, S. M. (1999). Bone resorption induced by parathyroid hormone is strikingly diminished in collagenase-resistant mutant mice. *J. Clin. Invest.* **103**, 517-524.

Zhao, W., Byrne, M. H., Wang, Y. and Krane, S. M. (2000). Osteocyte and osteoblast apoptosis and excessive bone deposition accompany failure of collagenase cleavage of collagen. *J. Clin. Invest.* **106**, 941-949.

Zijlstra, A., Aimes, R. T., Zhu, D., Regazzoni, K., Kupriyanova, T., Seandel, M., Deryugina, E. I. and Quigley, J. P. (2004). Collagenolysis-dependent angiogenesis mediated by matrix metalloproteinase-13 (collagenase-3). *J. Biol. Chem.* **279**, 27633-27645.